Enumeration of rare cells in whole blood by signal ion emission reactive release amplification (SIERRA) with same-sample RNA analysis

Zane Baird*†, Zehui Cao†, M. Regina Barron†‡, Anna Vorsilak†, Frédérique Deiss‡, and Michael Pugia†

†Single Cell Analytics Center, Indiana Biosciences Research Institute, Indianapolis, Indiana 46202, United States

‡Department of Chemistry & Chemical Biology, Indiana University - Purdue University Indianapolis, Indianapolis, Indiana 46202, United States

ABSTRACT: Herein is presented a platform capable of detecting less than 30 cells from a whole blood sample by size-exclusion filtration, microfluidic sample handling, and mass spectrometric detection through signal ion emission reactive release amplification (SIERRA). This represents an approximate 10-fold improvement in detection limits from previous work. Detection by SIERRA is accomplished through the use of novel nanoparticle reagents coupled with custom fluidic fixtures for precise sample transfer. Sample processing is performed in standardized 96-well microtiter plates with commonly available laboratory instrumentation to facilitate assay automation. The detection system is easily amenable to multiplex detection and compatibility with PCR-based gene assays is demonstrated.

Advancements in microfluidics and nanotechnology are driving analytics toward single-cell sensitivity and increased specificity[1–10]. Despite numerous developments, the detection and enumeration of rare cells in biological fluid remains clinically challenging due to the high background of non-rare cells (>10^9 cells/mL) and difficulties associated with sample handling[11–13]. Microfluidic filtration technologies have allowed for the automated capture and detection of circulating tumor cells (CTCs) based on size-exclusion filtration, coupled with immunocytochemistry (ICC) and analysis by microscopic fluorescent imaging[14]. Limited multiplexing capability, lengthy analysis times, and relatively low sample throughput have however been barriers to the adoption of such methodologies in clinical diagnostic laboratories. This is due in part to the need to remove leukocytes to levels such that immunoaffinity stained CTCs may be distinguished from the background population. Immunoaffinity-based enrichment such as that utilized by the CellSearch™ system, have routinely demonstrated the detection of a single cell in a 7.5 mL sample of blood, yet the sample processing is time consuming and the interpretation of results requires manual review of images[15,16]. Consequently, throughput is limited to approximately 8 samples per day. Flow cytometry-based ICC methodologies have also been applied to the detection of CTCs but instrumental cost and difficulties in instrument calibration to distinguish cells which comprise <0.0001% of the total population severely limit its utility[17].

While ICC has shown great promise in the detection and phenotyping of CTCs, the development of personalized treatments relies on genetic analysis of tumor material[18,19]. As such, CTC detection methods should ideally be non-destructive to oligonucleotides as well as allow for simple transfer of genetic material from isolated cells to allow processing by polymerase chain reaction (PCR) to amplify and sequence genetic material. Previous work has demonstrated the analysis of nucleic acids from 1-100 cells[20–22], yet removal of genetic materials from filtration membranes for analysis remains time-consuming and laborious. Maximization of throughput in a clinical laboratory necessitates screening methods to quickly identify samples which may be further subjected to genetic characterization and which allow for simple processing and transfer of genetic material for analysis with standard laboratory instrumentation. Furthermore, analysis of rare cells requires that the same sample aliquot used for screening may be subject to genetic analysis.

Detection by ICC is typically reliant on enzyme turnover, direct fluorescent labeling, or chemiluminescent signal transduction through conjugation of appropriate moieties with detection antibodies[23]. While these transduction methodologies exhibit good sensitivity for CTC detection, they are limited in multiplexing capacity due to spectral overlap and the time required for analysis. The lack of multiplexing capacity is particularly problematic as CTC identification generally requires the presence and/or absence of several markers for classification[24,25]. Additionally, quantification of ICC results is difficult, if not impossible in most cases. Assays which make use of optically encoded beads or spatially ordered arrays of capture antibodies allow for highly multiplexed, quantitative analysis within the same sample[26–28], but are limited to use with culture supernatant or lysed cells.

Unlike optical detection, mass spectrometry (MS) is capable of measuring hundreds to thousands of analytes within a single sample volume. Isobaric tagging of digested peptides has further advanced this detection method by allowing simultaneous sample processing which greatly decreases chromatographic separation time and allows for relative and absolute quantitation within a sample set[29–31]. In the case of protein expression, however, MS generally requires chromatography to achieve acceptable sensitivity, which

This is the author's manuscript of the article published in final edited form as:
Baird, Z., Barron, M. R., Cao, Z., Vorsilak, A., Deiss, F., & Pugia, M. (2019). Enumeration of rare cells in whole blood by signal ion emission reactive release amplification (SIERRA) with same-sample RNA analysis. Analytical Chemistry. https://doi.org/10.1021/acs.analchem.8b04446

significantly limits throughput. Mass cytometry has demonstrated measurement of >30 markers on a single cell without chromatographic separation[32,33] but requires hundreds of cells for meaningful analysis[34], has a recovery rate of <50% during sample pre-processing[35], and all cellular material is destroyed during analysis. We have previously demonstrated the use of particles coupled with cleavable mass labels and detection antibodies for the non-destructive enumeration of tumor cells[36]. While effective, this method is not amenable to high-throughput screening and recovery of genetic material for analysis is cumbersome at best.

Through a novel microfluidic filtration apparatus, we demonstrate the enrichment, non-destructive MS-based enumeration, and analysis of RNA from tumor cells from a single sample aliquot. The filtration apparatus makes use of 96-well plates and commonly available laboratory equipment for all sample processing steps to permit implementation within existing high-throughput laboratory workflows. Furthermore, the use of microtiter plates permits a blood sample to be easily aliquoted between multiple wells, thus reducing the effective background of non-rare cells for each individual measurement while allowing for simultaneous processing. Detection and enumeration of captured cells are enabled using novel nanoparticle (NP) reagents which employ signal ion emission reactive release amplification (SIERRA) to quantify cells based on immunostaining of surface proteins. Filtration-based enrichment of stained cells, followed by chemical cleavage of labels for MS based quantitation by nanoelectrospray ionization (nanoESI) is demonstrated. This detection methodology is shown to be compatible with downstream analysis of RNA from isolated cells.

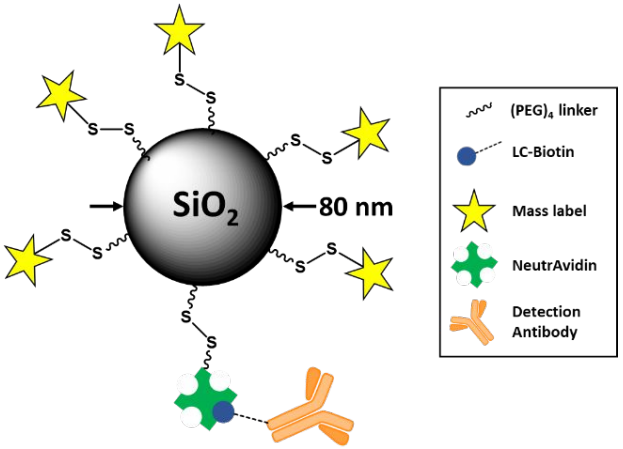

Figure 1: Schematic representation of SIERRA NP design

The SIERRA NPs are comprised of two principle entities: chemically cleavable mass labels and NeutrAvidin biotin-binding protein which functions as a modular method of coupling biotinylated detection antibodies to NPs. A schematic of SIERRA NP design is shown in Figure 1. Each SIERRA NP is decorated with mass labels to provide approximately 2.2×10^4 fold amplification from a single particle (see SI, section 2). We demonstrate the use of an internal standard (IS) sharing the same parent *m/z* as the mass label (isobaric) for quantitation by tandem MS. This strategy has the potential for increased multiplexing capacity by performing quantitative measurements of unique mass labels in overlapping MS spectral regions; however, a demonstration of multiplexing is beyond the scope of this manuscript and will be addressed in future work For this work, the inclusion of fluorescent tags on detection antibodies and NeutrAvidin allow for confirmation of SIERRA NP reactivity towards the target cells and serve as verification of NP binding to monoclonal antibody (mAb) through the NeutrAvidin-biotin interaction.

MATERIALS AND METHODS

Anhydrous dimethyl sulfoxide (DMSO), Sulfo-NHS-LC-Biotin (long chain biotin), EZ-link™ Dylight 488, EZ-link™ Dylight 550, EZ-link™ Dylight 650, NeutrAvidin, 2-Pyridyldithiol-tetraoxatetradecane-*N*-hydroxysuccinimide (PEG_4SPDP), and *N*-succinimidyl S-acetyl(thiotetraethyleneglycol) ($SAT(PEG)_4$) were acquired from Thermo Fisher Scientific (Waltham, MA, U.S.A.). Aminated silica NPs, polycarbonate track-etched (PCTE) membranes, and bottomless 96-well microtiter plates were purchased from Nanocomposix (San Diego, CA, U.S.A.), Sterlitech (Kent, WA, U.S.A.), and Greiner Bio-one (Kremsmünster, Austria), respectively. All fluorescent images were acquired with a Lionheart FX Live Cell Imager with Gen5 software (Biotek, Winooski, VT, U.S.A.) outfitted with LED and filter cube sets for DAPI, RFP, GFP, and CY5. All images were taken using phase-contrast objectives. Mass spectrometry was performed using an LTQ-XL (Thermo Fisher Scientific). NanoESI spray tips were pulled from 1.5 mm OD × 0.86 mm OD borosilicate capillaries (Sutter Instruments, Novato, CA, U.S.A.) on a Sutter Instruments P-1000 Micropipette Puller to a final tip diameter of 3-5 µm. Hydroxylamine HCl, ethylenediaminetetraacetic acid (EDTA), phosphate buffered saline (PBS), tris buffered saline (TBS), bovine serum albumin (BSA), tris(2-carboxyethyl)phosphine (TCEP), 4′,6-diamidino-2-phenylindole (DAPI), and all other reagents were purchased from Fisher Scientific unless otherwise noted. AC-5 and AC-5-2 peptides (mass label and internal standard, respectively) were supplied by Celtek (Franklin, TN, U.S.A) at a purity greater than 95%. See SI, section 4 for details on peptide structure and sequence. SKBR3 cells (ATCC HTB-30) were acquired from ATCC (Manassas, VA U.S.A.) and cultured in McCoy's 51 medium supplemented with 10% fetal bovine serum. Cultured cells were fixed with 2% paraformaldehyde and stored in PBS at 4 °C until use. Before use stock solutions of fixed SKBR3 cells were passed through a 30 µm CellTrics mesh filter (Sysmex, Norderstedt, Germany) and counted via hemocytometry.

Antibody production & conjugation

Mouse monoclonal antibodies targeting Her2/NEU and leukocyte common antigen (CD45) were produced from hybridomas purchased from ATCC (HB-10205 and HB-10508, respectively) and purified on an ÄKTA Prime with a HiTrap MabSelect SuRe Protein A column (GE Healthcare, Chicago, IL). The purified anti-Her2/NEU mAb was biotinylated by conjugation via amine-reactive crosslinking with sulfo-NHS-LC-Biotin and EZ-link™ Dylight 550, the product hereafter referred to as Her2-Dy550-LC-B. Similarly, anti-CD45 mAb was conjugated by reaction with EZ-link™ Dylight 650. NeutrAvidin was first reacted with EZ-link™ Dylight 488 NHS ester and further functionalized with a protected sulfhydryl moiety by reaction with $SAT(PEG)_4$. All coupling procedures

were performed according to product documentation and desalted with Illustra NAP-25 columns (GE Healthcare, Chicago, IL).

Nanoparticle preparation

A suspension of aminated silica NPs at a concentration of 20 mg/mL in PBS was first reacted with PEG_4SPDP to introduce a poly(oxyethylene) (PEG) linked sulfhydryl-reactive 2-pyridyldithio group. Following this reaction, the particles were washed and resuspended in DMSO. Unless otherwise noted, all wash steps involved centrifugation at 7000 ×g for 12 min followed by removal of supernatant, addition of fresh solvent or buffer, and resuspension of pelleted NPs via sonication for 30 s at 20% amplitude using a Q500 sonicator with 1/16" probe tip (Qsonica, Newtown, CT).

Free thiols were formed on the previously prepared NeutrAvidin conjugate by deacetylation with a solution of 0.5 M hydroxylamine, 25 mM EDTA in PBS. The deacetylated NeutrAvidin was desalted and buffer-exchanged into citrate-phosphate buffer (pH 4.5) with a NAP-25 column. Mass label peptide (AC-5) was dissolved in citrate-phosphate buffer and added to the deacetylated NeutrAvidin. The NP suspension in DMSO was added dropwise to this solution while stirring and the mixture was allowed to incubate on a nutating mixer overnight at room temperature. The suspension was then washed twice with a solution of water containing 0.1% formic acid and 0.2% Triton X-100, followed by three washes with 0.1% formic acid in water. Finally, the particles were resuspended in type I water, passed through a 10 µm CellTrics nylon-mesh filter and stored at 4 °C protected from light until use.

Immunostaining procedure

Approximately 8 mL of whole blood was collected from healthy donors into Circulating Tumour Cell TransFix®/EDTA Vacuum Blood Collection Tubes (Cytomark, Buckingham, UK) and was stored for 24-120 hours at room temperature before analysis. Blood tubes were inverted 5 times to ensure complete mixing and 35 µL aliquots were added to separate wells of a low binding microtiter plate. Five microliters of SKBR3 cell spike solution in PBS were added to the blood 2 hrs before the addition of SIERRA NPs. SIERRA NPs were functionalized with mAb by incubation at room temperature in Candor The Blocking Solution (CANDOR Bioscience GmbH, Wangen, Germany) for 1 hour with Her2-Dy550-LC-B (1:1 molar equivalent of mAb to NeutrAvidin on NPs) to introduce anti-Her2/NEU detection antibody. The suspension of mAb functionalized NPs was then filtered through a 1.0 µm PCTE membrane. The use of 1:1 mAb:NeutrAvidin was to assure that free mAb would be efficiently bound by NPs as each NeutrAvidin is typically capable of binding up to 4 biotin molecules. Immunostaining of cells in whole blood was initiated by the addition of 10 µL of a mixture containing anti-Her2/NEU-dy550-LC-B functionalized SIERRA NPs and anti-CD45-Dy650 for a final concentration of 200 µg/mL and 15 µg/mL, respectively. This suspension was incubated for 1 hour at room temperature before filtration was performed. The reactivity of anti-her2/NEU SIERRA NPs towards SKBR3 cells spiked in whole blood was verified through fluorescent imaging after enrichment by filtration. A composite image of the staining is shown in Figure 2. This image illustrates the specificity of the prepared SIERRA NPs towards SKBR3 cells in the presence of background cells.

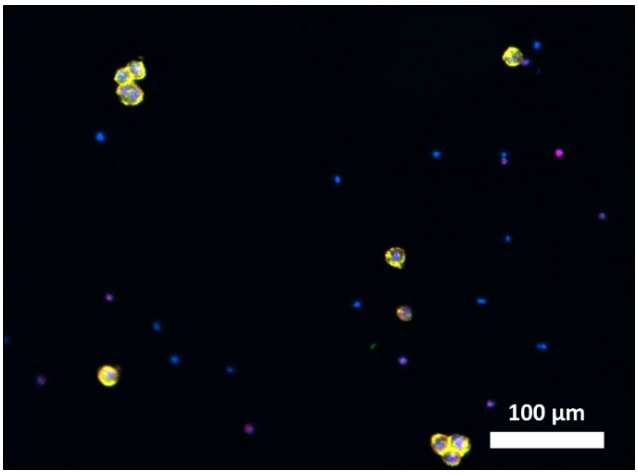

Figure 2: Composite image of a filtration-enriched sample of whole blood containing SKBR3 cells. Sample was immunostained with SIERRA NPs targeting Her2/NEU (green/orange)), DAPI nuclear stain (blue), and CD45 (violet). Overlap of green and orange fluorescence on NeutrAvidin and anti-Her2/NEU, respectively, results in yellow coloration seen on cells stained by SIERRA NPs.

Filtration of stained samples

All samples were filtered simultaneously through individual wells of a 96-well filtration apparatus consisting of a bottomless microtiter plate with an adhered 8.0 µm PCTE membrane. Prior to use, each well was blocked with a solution of 1% BSA in PBS overnight at 4 °C. Negative pressure for filtration was provided by the vacuum manifold of a EL406 plate washer (Biotek, VT, U.S.A). Processing of each sample involved the following: 1) 50 µL of PBS was added to the well containing the immunostained blood and the resulting dilute blood solution was filtered in a single aliquot through a single well of the 96-well filter plate; 2) each well was rinsed twice with 100 µL of wash buffer (10% Candor The Blocking Solution, 0.05% Tween-20 in PBS) and the wash volume filtered through its respective well on the filtration plate; 3) each well of the filtration membrane was then washed with 100 µL of fresh wash buffer; 4) 50 µL of 1 µg/mL DAPI in PBS was applied to the cells isolated on the membrane and allowed to incubate for 1 min at room temperature; 5) filtration membrane washed 5 times with 200 µL of 10 mM ammonium acetate pH 5.6. The 96-well filter plate was then removed from the manifold and the bottom of the membrane was rinsed with a stream of deionized water for 30 seconds.

Fluorescent imaging and cell counting

Following filtration, the cells isolated on the membrane were subjected to automated fluorescent imaging by microscopy. For each well a series of fluorescent images were taken in DAPI, GFP, RFP, and CY5 channels at 4X magnification. The images were processed with Gen5 software to produce a single stitched

image for each well of the filtration membrane. Each of the stitched images was then analyzed using Gen5 software to determine a true SKBR3 cell count from fluorescence originating from anti-Her2/NEU-dy550-LC-B. Details on imaging parameters and instrumental settings used for automated cell counting are given in SI, section 3.

Analysis of filtered cells by mass spectrometry

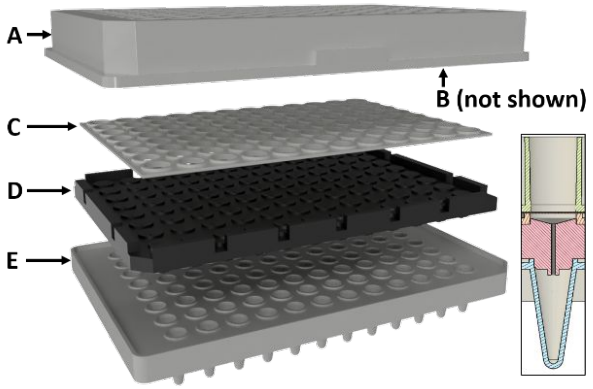

Figure 3: Exploded view of fluidic transfer apparatus with (A) bottomless microtiter plate with (B) attached PCTE membrane, (C) silicone gasket, (D) aluminum fluidic transfer plate, and (E) 96-well sample collection plate. Inset image is a cross-section view of single well of fluidic transfer apparatus.

The filtration plate used to isolate cells from blood samples was assembled with a silicone gasket, aluminum fluidic transfer plate, and a 96-well polypropylene (PP) sample collection plate as shown in Figure 3 to form the sample transfer assembly. All components of the sample transfer assembly were designed and manufactured in house. Fifty microliters of a solution containing 5 mM TCEP, 50 nM AC-5-2, and 10 mM ammonium acetate was added to each well of the filtration plate to initiate cleavage of MS labels from bound NPs. The filtration plate was sealed with an adhesive-backed plate sealer and allowed to rest at room temperature for 30 min. The adhesive

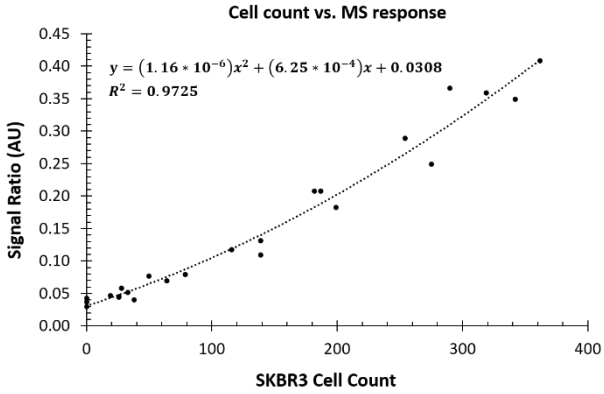

Figure 4: MS response vs. SKBR3 cell count from whole blood samples immunostained with SIERRA NPs. NPs were functionalized with AC-5 mass label and Her2-Dy550-LC-B. Response is plotted as the ratio of signal from AC-5 mass label to AC-5-2 internal standard. Cell counting was automated from stitched fluorescent images

plate sealer was removed, and the sample transfer assembly was centrifuged for 2 min at 200 ×g to facilitate the full transfer of solution containing cleaved MS labels into the 96-well PP collection plate. For each sample, 8 µL of solution from the collection plate was loaded into a pulled borosilicate nanospray emitter. Spray voltage was applied through a silver wire inserted into the back of the emitter and MS/MS spectra were collected at *m/z* 618.5 for 15 seconds (see SI, section 1 for full MS/MS parameters). The average ratio of intensities of fragments *m/z* 308 and *m/z* 322 for each sample were then plotted versus cell counts obtained by microscopy to construct a response curve. The ratio of intensities is represented by "Signal Ratio" in all plots.

RNA analysis

After analysis of filtered samples by fluorescent microscopy and MS, the filtration membrane for each sample well selected for RNA analysis was removed and placed in a 0.5 mL centrifuge tube. To each tube, 50 µL of lysis buffer containing TBS with 0.5% NP-40 and 20 µg proteinase K was added. The solution was incubated at 55 °C for 60 min for proteinase K digestion, followed by a 15 min incubation at 65 °C to reverse formaldehyde crosslinking. The temperature was then raised to 80 °C for 15 min to deactivate the protease. The processed sample was immediately used as a template for reverse-transcription quantitative polymerase chain reaction (RT-qPCR) analysis or stored at -80 °C.

A RT-qPCR TaqMan™ assay was developed for multiplex detection of mRNAs of cytokeratin (CK19) and beta-actin (ACTB) using the following primers and probes from Integrated DNA Technologies (Skokie, Illinois): for CK19, forward primer: 5'-CACTACTACACGACCATCC-3', reverse primer: 5'-ATCCTGGAGTTCTCAATGGT-3', probe: 5'-FAM-CTGCGGGACAAGATTCTTGGTGCC- ZEN-Iowa Black® quencher-3'; for ACTB, forward primer: 5'-CGAGAAGATGACCCAGATCA-3', reverse primer: 5'-GATAGCACAGCCTGGATAG-3', probe: 5'-HEX-ACCTTCAACACCCCAGCCATGTAC- ZEN-Iowa Black® quencher-3'. The reverse primers were also used as the primers for cDNA synthesis during reverse transcription.

The RT-qPCR reaction was conducted using the Luna Universal Probe One-step RT-qPCR kit (New England Biolabs, MA). The PCR reaction solution (20 µL) contained forward and reverse primers (0.4 µM), dye and quencher labeled probe (0.2 µM), BSA (1 mg/mL), and 2 µL of template. The reaction was run on the QuantStudio3 real-time PCR instrument (Applied Biosystems, CA) using TaqMan™ chemistry, standard curve experiment, and a program of 55°C for 10 min, 95°C for 1 min for 1 cycle, and then cycling at 95°C for 10 sec followed by 15 sec at 60°C for up to 55 cycle, and finally storing the sample at 4°C. Positive and negative controls containing and lacking SKBR3 were run. The cycle threshold (Ct) values were determined using amplification plots for CK19 and ACTB mRNA by the QuantStudio™ Design & Analysis Software and were then used to calculate the detection limits for the measurement of SKBR3 cells added to whole blood. Lower Ct signifies higher initial template concentration, and one cycle difference in Ct indicates a measurable 2-fold difference in concentration. A more detailed discussion of considerations on the assay design is given in SI, section 5.

RESULTS & DISCUSSION:

SKBR3 enumeration by MS

Serial dilutions of fixed SKBR3 cells in PBS were prepared for use as spiking solutions. These standards were spiked into whole blood, stained with anti-Her2NEU functionalized SIERRA NPs, enriched by filtration, and subject to analysis by MS and fluorescent imaging according to procedures outlined in previous sections. Fluorescent imaging data was used to determine the actual cell count due to account for variability in the preparation of solutions containing a relatively low number of cells. The resulting plot of the MS response vs. cell count as determined from fluorescent imaging is shown in Figure 4.

The observed trend seems to indicate a non-linear response with increasing numbers of cells and as such the response curve was generated with a second order polynomial fit. The most likely reason for this non-linearity is error in automated cell count by fluorescent microscopy. As the concentration of SKBR3 cells isolated on the membrane increases, the algorithm is no longer able to distinguish single cells from clusters due to overlap. The result is a fluorescent cell count that has an inherent low-bias as the concentration of cells increases on the membrane. One possible source of error in the quantitation by SIERRA is the binding of multiple antibodies by a single NeutrAvidin molecule; however, good correlation between cells counted by microscopy and quantitative MS results indicates that the probability of such an event is low.

SIERRA-MS limit of detection

The lower limit of detection (LOD) was determined by preparing eight replicates containing approximately 50 cells and six blank solutions according to immunostaining and filtration procedures outlined in Materials and Methods. In addition, two blank samples were processed without inclusion of SIERRA NPs to analyze the background contribution to blank signals and verify that non-specific binding was not a major contribution in blank response. Cell counts from fluorescent images were used to determine the actual number of SKBR3 cells isolated during filtration and manual review of the fluorescent images was conducted to ensure validity of automated cell counts. The plot of MS response vs. isolated cell count is shown in Figure 5.

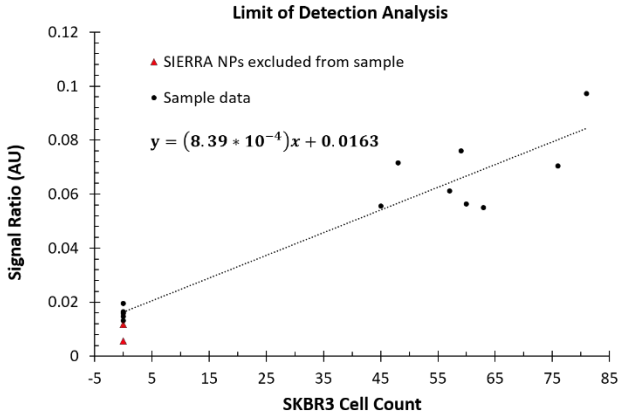

Figure 5: MS response vs. SKBR3 cell count from whole blood samples immunostained with SIERRA NPs (black circles). NPs were functionalized with AC-5 mass label and Her2-Dy550-LC-B. Response is plotted as the ratio of signal from AC-5 mass label to AC-5-2 internal standard. Red triangles are samples processed without SIERRA NPs. Linear regression analysis did not include samples processed without SIERRA NPs

The limit of detection (LOD) and limit of quantitation (LOQ) can be calculated according to Equations 1 and 2 where $\bar{x}_0$, σ_0, and $\bar{x}$ are the mean blank response, standard deviation of the blank response, and mean response per cell, respectively[37].

$$LOD = \frac{\bar{x}_0 + 3\sigma_0}{\bar{x}} \quad \text{Eq. 1}$$

$$LOQ = \frac{\bar{x}_0 + 10\sigma_0}{\bar{x}} \quad \text{Eq. 2}$$

A least squares linear regression analysis of the data in Figure 5 was performed and $\bar{x}$ and $\bar{x}_0$ are represented by the resulting slope (8.39×10^{-4}) and y-intercept (1.63×10^{-2}), respectively. Applying the calculated values to Eq. 1 and Eq. 2 along with the computed σ_0 (1.93×10^{-3}) results in an LOD of ~26 cells and an LOQ of ~42 cells. The LOD achieved in this work represents an increase in sensitivity of approximately 10-fold when compared to previous work using SIERRA for the detection of SKBR3 cells in whole blood[36].

Compatibility with transcript analysis

Fixatives in the TransFix® tubes protect cellular RNA from complete degradation; however, fixed RNA is not compatible with reverse transcription for RT-qPCR analysis. To address this, a sample pretreatment step was adopted using elevated temperature in the presence of tris buffer to reverse crosslinking of RNA, as previously reported[38]. We found that compared to treated samples, untreated fixed samples had about 100x lower mRNA detected in RT-qPCR (data not shown), suggesting the fixation reversing step is critical for RNA analysis. Despite the stabilizing effect of RNA crosslinking, the fixation and reversing processes are known to cause some RNA degradation. By simply modifying the RT-qPCR design to detect a 70-base long target region within the previously longer 130-base sequence, Ct values dropped 4-fold on average (data not shown), indicating significant fragmentation with 16-fold more mRNA fragments containing more than 70 bases compared to any fragments over 130 bases in length. Shorter target sequences would likely result in higher fragment coverage but were not pursued here due to considerations in assay design.

As a demonstration of the compatibility of PCR-based assays following SIERRA-MS detection, SKBR3 cells were spiked into PBS at varying levels, the solutions immunostained with SIERRA NPs, enriched by filtration, subjected to MS analysis procedures and finally CK19 and ACTB mRNA analysis was performed according to procedures outlined in Materials and Methods. The mRNAs of both genes were detected for as low as about 300 SKBR3 cells, with Ct values similar to those obtained from SKBR3 cells that did not undergo SIERRA-MS analysis. These results indicate the procedures used to treat cells on the membrane for MS analysis did not remove or damage genetic materials including mRNA inside the cells, and thus did not interfere with the transcript analysis. Our approach has clearly demonstrated the capability of the SIERRA platform to integrate multiple assays into a single system for reduced sample processing and faster turnaround time.

Sample throughput and practical limitations

Two of the primary concerns with any CTC detection method are the throughput and ability to distinguish CTCs from non-rare cells. According to product literature, CellSearch™ – the only FDA approved CTC detection platform – is capable of processing eight tubes of blood (60 mL total) in parallel in approximately three hours; however, this does not include the necessary time for manual review of the images to confirm detected CTCs. To address these concerns an additional study was performed in which 750 µL aliquots of blood were spiked with varying levels of SKBR3 cells, immunostained with SIERRA NPs, and filtered through single wells of the microtiter filtration plate as described in SI, section 6. The resulting MS response curve (Figure S2) shows good linearity over the same range tested previously (Figure 4) despite more than a 21-fold increase in sample processing volume through the same membrane area. These results highlight the robustness of the SIERRA methodology in the specific detection of cell-surface markers. It should be noted that this study utilized a separate batch of SIERRA NPs which were functionalized with ~ 30% more MS label and in addition with ~5-fold greater loading of NeutrAvidin in comparison to NPs used in the previous experiments.

Given the ability to process at least 750 µL of blood per well of the filtration apparatus, eight separate 7.5 mL tubes of blood can be simultaneously processed on a single 96-well microtiter plate with an additional 16 wells available for calibration standards. It is estimated that eight tubes of blood can be processed on a single 96-well plate in less than two hours with the use of an automated plate washer and MS injection by autosampler. This throughput is easily enhanced through parallel immunostaining of samples to be run on multiple plates as incubation with SIERRA NPs is the longest step in the process (one hour). Additionally, the use of standard microtiter plate format maintains compatibility with existing laboratory automation technology, permitting ease of adoption in existing clinical labs without the need for new instrumentation.

The usage of NP reagent can be a concern given the current method of staining cells in a large volume of blood, prior to isolation by filtration. Future work will aim to reduce the amount of reagent required by first performing enrichment of unstained cells on the membrane followed by staining with SIERRA NPs in a much smaller solution volume. This approach has had success in previous studies based on ICC[14], but requires retention of solution on the membrane for up to one hour which is not feasible with the current filtration plates. Through a specially engineered plate we expect to address this concern, but this is not in the scope of the present work.

Another important consideration observed in this work is the storage time of blood in TransFix® tubes and its effect on quantifiable immunostaining by SIERRA NPs. Initial experiments indicate that increased storage time increases background levels in blank samples which could negatively impact detection limits. This is especially true when processing larger volumes of blood in which non-rare cells enriched to higher numbers on the filtration membrane. We hope to address this issue in future studies by the inclusion of calibrators to account for varying sample matrices and allow for a robust method of absolute quantitation which is not reliant on microscopy.

CONCLUSIONS AND OUTLOOK:

In summary, we have developed a highly-sensitive rare cell detection platform which is easily amendable to high-throughput screening due to the use of standard format microtiter plates and ordinary laboratory equipment for sample processing. The results presented show that a population of cells comprising <1 ppm of the total can be distinguished and characterized based on antigenicity in a truly automatable fashion. Novel nanoparticle reagents decorated with cleavable labels and detection antibodies are shown to provide the capability to quantify antibody binding response through signal transduction by the release of mass labels from as few as 42 immunostained cells with limits of detection as low as 26 cells. The use of MS for detection avoids problems associated with spectral overlap which has traditionally limited multiplexed analysis relying on optical detection. Furthermore, our use of an isobaric internal standard serves as a demonstration that otherwise indistinguishable spectral peaks can be used to encode greater multiplexing capacity within a given MS detection window through the employment of tandem MS. While it is beyond the scope of this study, future work aims to demonstrate multiplexed analysis using SIERRA technology.

The rare cell analysis platform herein was also demonstrated to be non-destructive and directly compatible with fluorescent imaging as well as with preparation and analysis of genetic material by PCR following the release of MS labels. The latter capability is invaluable as genetic analysis of rare cells – such as CTCs – is paramount in the development of personalized therapies and understanding of underlying disease processes. Despite the wider availability and diminishing cost of molecular sequencing, its price remains high compared to many analytical methods. As such, systems capable of screening to select samples for further characterization are essential for efficient usage of resources. The technology demonstrated within this work is especially applicable for screening samples for which there is limited availability and thus demand strict sample conservation. Through highly sensitive and non-destructive isolation and characterization of cells by the methods presented we hope to address this screening niche and move towards a better understanding of biological processes at the single cell level.

ACKNOWLEDGMENTS

The authors would like to thank Dr. Carmella Evans-Molina, MD, PhD of Indiana University School of Medicine for providing the blood samples used in assay development.

SUPPORTING INFORMATION

Additional experimental methods and results

REFERENCES

(1) Brouzes, E.; Medkova, M.; Savenelli, N.; Marran, D.; Twardowski, M.; Hutchison, J. B.; Rothberg, J. M.; Link, D. R.; Perrimon, N.; Samuels, M. L. Droplet Microfluidic Technology for Single-Cell High-Throughput Screening. *Proc. Natl. Acad. Sci. U.S.A.* **2009**, *106* (34), 14195.

(2) Wheeler, A. R.; Throndset, W. R.; Whelan, R. J.; Leach, A. M.; Zare, R. N.; Liao, Y. H.; Farrell, K.; Manger, I. D.; Daridon, A. Microfluidic Device for Single-Cell Analysis. *Anal. Chem.* **2003**, *75* (14), 3581–3586. https://doi.org/10.1021/ac0340758.

(3) White, A. K.; VanInsberghe, M.; Petriv, O. I.; Hamidi, M.; Sikorski, D.; Marra, M. A.; Piret, J.; Aparicio, S.; Hansen, C. L. High-Throughput Microfluidic Single-Cell RT-QPCR. *Proc. Natl. Acad. Sci. U.S.A.* **2011**, *108* (34), 13999.

(4) Mazutis, L.; Gilbert, J.; Ung, W. L.; Weitz, D. A.; Griffiths, A. D.; Heyman, J. A. Single-Cell Analysis and Sorting Using Droplet-Based Microfluidics. *Nat. Protoc.* **2013**, *8*, 870–891.

(5) Klein, A. M.; Mazutis, L.; Akartuna, I.; Tallapragada, N.; Veres, A.; Li, V.; Peshkin, L.; Weitz, D. A.; Kirschner, M. W. Droplet Barcoding for Single-Cell Transcriptomics Applied to Embryonic Stem Cells. *Cell* **2015**, *161* (5), 1187–1201. https://doi.org/10.1016/j.cell.2015.04.044.

(6) Lecault, V.; White, A. K.; Singhal, A.; Hansen, C. L. Microfluidic Single Cell Analysis: From Promise to Practice. *Curr. Opin. Chem. Biol.* **2012**, *16* (3), 381–390. https://doi.org/10.1016/j.cbpa.2012.03.022.

(7) Zhao, X.; Hilliard, L. R.; Mechery, S. J.; Wang, Y.; Bagwe, R. P.; Jin, S.; Tan, W. A Rapid Bioassay for Single Bacterial Cell Quantitation Using Bioconjugated Nanoparticles. *Proc. Natl. Acad. Sci. U.S.A.* **2004**, *101* (42), 15027–15032. https://doi.org/10.1073/pnas.0404806101.

(8) Kneipp, K.; Haka, A. S.; Kneipp, H.; Badizadegan, K.; Yoshizawa, N.; Boone, C.; Shafer-Peltier, K. E.; Motz, J. T.; Dasari, R. R.; Feld, M. S. Surface-Enhanced Raman Spectroscopy in Single Living Cells Using Gold Nanoparticles. *Appl. Spectrosc.* **2002**, *56* (2), 150–154. https://doi.org/10.1366/0003702021954557.

(9) Chang, Y.-C.; Yang, C.-Y.; Sun, R.-L.; Cheng, Y.-F.; Kao, W.-C.; Yang, P.-C. Rapid Single Cell Detection of Staphylococcus Aureus by Aptamer-Conjugated Gold Nanoparticles. *Sci. Rep.* **2013**, *3*, 1863.

(10) Yang, Y.-S. S.; Atukorale, P. U.; Moynihan, K. D.; Bekdemir, A.; Rakhra, K.; Tang, L.; Stellacci, F.; Irvine, D. J. High-Throughput Quantitation of Inorganic Nanoparticle Biodistribution at the Single-Cell Level Using Mass Cytometry. *Nat. Commun.* **2017**, *8*, 14069.

(11) Yu, M.; Stott, S.; Toner, M.; Maheswaran, S.; Haber, D. A. Circulating Tumor Cells: Approaches to Isolation and Characterization. *J. Cell Biol.* **2011**, *192* (3), 373–382. https://doi.org/10.1083/jcb.201010021.

(12) Understanding Your Complete Blood Count (CBC) and Common Blood Deficiencies https://www.cc.nih.gov/ccc/patient_education/pepubs/cbc.pdf (accessed Sep 18, 2018).

(13) Paterlini-Brechot, P.; Benali, N. L. Circulating Tumor Cells (CTC) Detection: Clinical Impact and Future Directions. *Cancer Lett.* **2007**, *253* (2), 180–204. https://doi.org/10.1016/j.canlet.2006.12.014.

(14) Magbanua, M. J. M.; Pugia, M.; Lee, J. S.; Jabon, M.; Wang, V.; Gubens, M.; Marfurt, K.; Pence, J.; Sidhu, H.; Uzgiris, A.; et al. A Novel Strategy for Detection and Enumeration of Circulating Rare Cell Populations in Metastatic Cancer Patients Using Automated Microfluidic Filtration and Multiplex Immunoassay. *PLoS One* **2015**, *10* (10), e0141166. https://doi.org/10.1371/journal.pone.0141166.

(15) Allard, W. J.; Matera, J.; Miller, M. C.; Repollet, M.; Connelly, M. C.; Rao, C.; Tibbe, A. G. J.; Uhr, J. W.; Terstappen, L. W. M. M. Tumor Cells Circulate in the Peripheral Blood of All Major Carcinomas but Not in Healthy Subjects or Patients With Nonmalignant Diseases. *Clin. Cancer Res.* **2004**, *10* (20), 6897–6904. https://doi.org/10.1158/1078-0432.CCR-04-0378.

(16) Coumans, F.; Terstappen, L. Detection and Characterization of Circulating Tumor Cells by the CellSearch Approach. In *Whole Genome Amplification: Methods and Protocols*; Kroneis, T., Ed.; Springer New York: New York, NY, 2015; pp 263–278. https://doi.org/10.1007/978-1-4939-2990-0_18.

(17) Khan, S. S.; Solomon, M. A.; McCoy, J. P. Detection of Circulating Endothelial Cells and Endothelial Progenitor Cells by Flow Cytometry. *Cytometry, Part B* **2005**, *64B* (1), 1–8. https://doi.org/10.1002/cyto.b.20040.

(18) Maheswaran, S.; Haber, D. A. Circulating Tumor Cells: A Window into Cancer Biology and Metastasis. *Curr. Opin. Genet. Dev.* **2010**, *20* (1), 96–99. https://doi.org/10.1016/j.gde.2009.12.002.

(19) Lynch, T. J.; Bell, D. W.; Sordella, R.; Gurubhagavatula, S.; Okimoto, R. A.; Brannigan, B. W.; Harris, P. L.; Haserlat, S. M.; Supko, J. G.; Haluska, F. G.; et al. Activating Mutations in the Epidermal Growth Factor Receptor Underlying Responsiveness of Non–Small-Cell Lung Cancer to Gefitinib. *N. Engl. J. Med.* **2004**, *350* (21), 2129–2139. https://doi.org/10.1056/NEJMoa040938.

(20) Krebs, M. G.; Metcalf, R. L.; Carter, L.; Brady, G.; Blackhall, F. H.; Dive, C. Molecular Analysis of Circulating Tumour Cells—Biology and Biomarkers. *Nat. Rev. Clin. Oncol.* **2014**, *11*, 129–144.

(21) Magbanua, M. J. M.; Sosa, E. V.; Scott, J. H.; Simko, J.; Collins, C.; Pinkel, D.; Ryan, C. J.; Park, J. W. Isolation and Genomic Analysis of Circulating Tumor Cells from Castration Resistant Metastatic Prostate Cancer. *BMC Cancer* **2012**, *12* (1), 78. https://doi.org/10.1186/1471-2407-12-78.

(22) Magbanua, M. J. M.; Sosa, E. V.; Roy, R.; Eisenbud, L. E.; Scott, J. H.; Olshen, A.; Pinkel, D.; Rugo, H. S.; Park, J. W. Genomic Profiling of Isolated Circulating Tumor Cells from Metastatic Breast Cancer Patients. *Cancer Res.* **2013**, *73* (1), 30–40. https://doi.org/10.1158/0008-5472.CAN-11-3017.

(23) Hermanson, G. T. *Bioconjugate Techniques*, 3rd ed..; Bioconjugate Techniques; London : Academic Press: London, 2013.

(24) Pugia, M.; Magbanua, M. J. M.; Park, J. W. Enrichment and Detection of Circulating Tumor Cells and Other Rare Cell Populations by Microfluidic Filtration. In *Isolation and Molecular Characterization of Circulating Tumor Cells*; Magbanua, M. J. M., Park, J. W., Eds.; Springer International Publishing: Cham, 2017; pp 119–131. https://doi.org/10.1007/978-3-319-55947-6_6.

(25) Alix-Panabières, C.; Pantel, K. Circulating Tumor Cells: Liquid Biopsy of Cancer. *Clin. Chem.* **2013**, *59* (1), 110. https://doi.org/10.1373/clinchem.2012.194258.

(26) Morgan, E.; Varro, R.; Sepulveda, H.; Ember, J. A.; Apgar, J.; Wilson, J.; Lowe, L.; Chen, R.; Shivraj, L.; Agadir, A.; et al. Cytometric Bead Array: A Multiplexed Assay Platform with Applications in Various Areas of Biology. *Clin. Immunol.* **2004**, *110* (3), 252–266. https://doi.org/10.1016/j.clim.2003.11.017.

(27) Vignali, D. A. A. Multiplexed Particle-Based Flow Cytometric Assays. *J. Immunol. Methods* **2000**, *243* (1), 243–255. https://doi.org/10.1016/S0022-1759(00)00238-6.

(28) Kingsmore, S. F. Multiplexed Protein Measurement: Technologies and Applications of Protein and Antibody Arrays. *Nat. Rev. Drug Discovery* **2006**, *5*, 310–321.

(29) Ross, P. L.; Huang, Y. N.; Marchese, J. N.; Williamson, B.; Parker, K.; Hattan, S.; Khainovski, N.; Pillai, S.; Dey, S.; Daniels, S.; et al. Multiplexed Protein Quantitation in Saccharomyces Cerevisiae Using Amine-Reactive Isobaric Tagging Reagents. *Mol. Cell. Proteomics* **2004**, *3* (12), 1154–1169. https://doi.org/10.1074/mcp.M400129-MCP200.

(30) Thompson, A.; Schäfer, J.; Kuhn, K.; Kienle, S.; Schwarz, J.; Schmidt, G.; Neumann, T.; Hamon, C. Tandem Mass Tags: A Novel Quantification Strategy for Comparative Analysis of Complex Protein Mixtures by MS/MS. *Anal. Chem.* **2003**, *75* (8), 1895–1904. https://doi.org/10.1021/ac0262560.

(31) Wiese, S.; Reidegeld, K. A.; Meyer, H. E.; Warscheid, B. Protein Labeling by ITRAQ: A New Tool for Quantitative Mass Spectrometry in Proteome Research. *Proteomics* **2007**, *7* (3), 340–350. https://doi.org/10.1002/pmic.200600422.

(32) Simoni, Y.; Chng, M. H. Y.; Li, S.; Fehlings, M.; Newell, E. W. Mass Cytometry: A Powerful Tool for Dissecting the Immune Landscape. *Curr. Opin. Immunol.* **2018**, *51*, 187–196. https://doi.org/10.1016/j.coi.2018.03.023.

(33) Bendall, S. C.; Simonds, E. F.; Qiu, P.; Amir, E. D.; Krutzik, P. O.; Finck, R.; Bruggner, R. V.; Melamed, R.; Trejo, A.; Ornatsky, O. I.; et al. Single-Cell Mass Cytometry of Differential Immune and Drug Responses Across a Human Hematopoietic Continuum. *Science* **2011**, *332* (6030), 687–696. https://doi.org/10.1126/science.1198704.

(34) Yao, Y.; Liu, R.; Shin, M. S.; Trentalange, M.; Allore, H.; Nassar, A.; Kang, I.; Pober, J. S.; Montgomery, R. R. CyTOF Supports Efficient Detection of Immune Cell Subsets from Small Samples. *J.*

Immunol. Methods **2014**, *415*, 1–5. https://doi.org/10.1016/j.jim.2014.10.010.

(35) Nassar, A. F.; Wisnewski, A. V.; Raddassi, K. Mass Cytometry Moving Forward in Support of Clinical Research: Advantages and Considerations. *Bioanalysis* **2016**, *8* (4), 255–257. https://doi.org/10.4155/bio.15.257.

(36) Baird, Z.; Pirro, V.; Ayrton, S.; Hollerbach, A.; Hanau, C.; Marfurt, K.; Foltz, M.; Cooks, R. G.; Pugia, M. Tumor Cell Detection by Mass Spectrometry Using Signal Ion Emission Reactive Release Amplification. *Anal. Chem.* **2016**, *88* (14), 6971–6975. https://doi.org/10.1021/acs.analchem.6b02043.

(37) Harris, D. C. Quality Assurance and Calibration Methods. In *Quantitative Chemical Analysis*; New York : W.H. Freeman and Co.: New York, NY, 2010; pp 84–87.

(38) Evers, D. L.; Fowler, C. B.; Cunningham, B. R.; Mason, J. T.; O'Leary, T. J. The Effect of Formaldehyde Fixation on RNA. *J. Mol. Diagn.* **2011**, *13* (3), 282–288. https://doi.org/10.1016/j.jmoldx.2011.01.010.

for TOC only

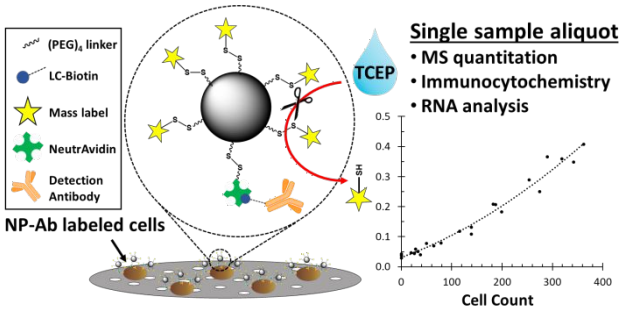
(PEG)4 linker
LC-Biotin
Mass label
NeutrAvidin
Detection Antibody
NP-Ab labeled cells
TCEP
SH
Single sample aliquot
• MS quantitation
• Immunocytochemistry
• RNA analysis
0.5
0.4
0.3
0.2
0.1
0.0
0
100
200
300
400
Cell Count